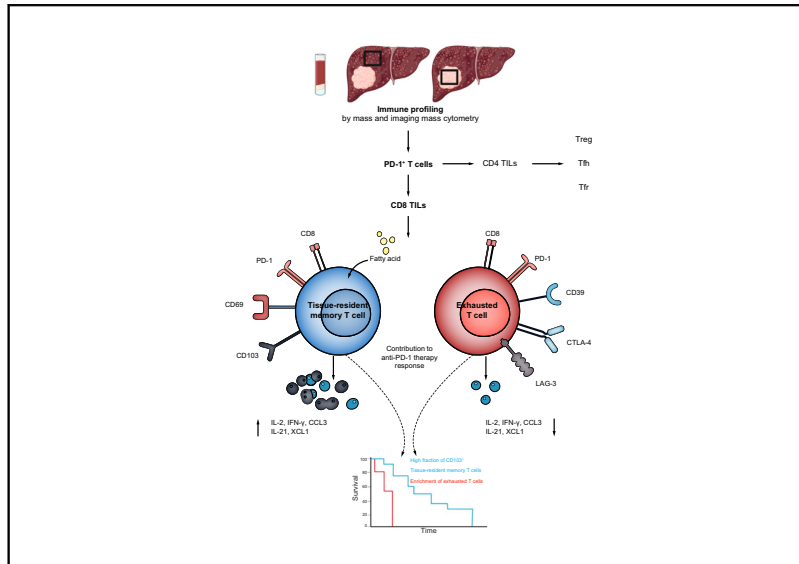Research Article
Hepatic and Biliary Cancer

T-cell exhaustion and residency dynamics inform clinical outcomes in hepatocellular carcinoma

Graphical abstract

Highlights

- In patients with HCC, exhausted T cells and CD103+ tissue-resident memory T cells have opposing roles.

- Enrichment of poorly functional PD-1+ exhausted T cells in the tumor tissue is associated with poor progression-free survival.

- Tissue-resident memory T cells have higher effector function and metabolic activity and are associated with longer survival.

- The balance between CD103+ tissue-resident and exhausted T cells can predict outcomes during PD-1 therapy.

Authors

Maryam Barsch, Henrike Salié, Alexandra Emilia Schlaak, …, Michael Schultheiss, Robert Thimme, Bertram Bengsch

Correspondence

bertram.bengsch@uniklinik-freiburg.de (B. Bengsch).

Lay summary

The role of the immune response in hepatocellular carcinoma (HCC) remains unclear. T cells can mediate protection against tumor cells but are frequently dysfunctional and exhausted in cancer. We found that patients with a predominance of exhausted CD8+ T cells (TEX) had poor survival compared to patients with a predominance of tissue-resident memory T cells (TRM). This correlated with the molecular profile, metabolic and functional status of these cell populations. The enrichment of TEX was independently associated with prognosis in addition to disease stage, age and tumor markers. A high TRM proportion was also associated with better outcomes following checkpoint therapy. Thus, these T-cell populations are novel biomarkers with relevance in HCC.

Research Article
Hepatic and Biliary Cancer

JOURNAL
OF HEPATOLOGY

T-cell exhaustion and residency dynamics inform clinical outcomes in hepatocellular carcinoma

Maryam Barsch[1], Henrike Salié[1], Alexandra Emilia Schlaak[1], Zhen Zhang[1], Moritz Hess[2], Lena Sophie Mayer[1], Catrin Tauber[1], Patricia Otto-Mora[1], Takuya Ohtani[3], Tobias Nilsson[1], Lara Wischer[1], Frances Winkler[1], Sasikant Manne[3], Andrew Rech[3], Annette Schmitt-Graeff[4], Peter Bronsert[4], Maike Hofmann[1], Christoph Neumann-Haefelin[1], Tobias Boettler[1], Stefan Fichtner-Feigl[5], Florian van Boemmel[6], Thomas Berg[6], Lorenza Rimassa[7,8], Luca Di Tommaso[7,9], Anwaar Saeed[10], Antonio D'Alessio[7,11], David J. Pinato[11,12], Dominik Bettinger[1], Harald Binder[2], E. John Wherry[3], Michael Schultheiss[1], Robert Thimme[1], Bertram Bengsch[1,13,14,*]

[1]University Medical Center Freiburg, Clinic for Internal Medicine II, Germany; [2]University Medical Center Freiburg, Institute for Medical Biometry and Statistics (IMBI), Germany; [3]University of Pennsylvania, Perelman School of Medicine, Institute for Immunology, USA; [4]University Medical Center Freiburg, Institute of Clinical Pathology, Germany; [5]University Medical Center Freiburg, Clinic for General and Visceral Surgery, Germany; [6]Leipzig University Medical Center, Division of Hepatology, Dpt. of Medicine II, Germany; [7]Department of Biomedical Sciences, Humanitas University, Pieve Emanuele, Milan, Italy; [8]IRCCS Humanitas Research Hospital, Humanitas Cancer Center, Medical Oncology and Hematology Unit, Rozzano (Milan), Italy; [9]Pathology Unit IRCCS Humanitas Research Hospital Rozzano, Milan, Italy; [10]Department of Medicine, Division of Medical Oncology, Kansas University Cancer Center, Kansas City, Kansas, USA; [11]Imperial College London, Faculty of Medicine, Department of Surgery & Cancer, UK; [12]Division of Oncology, Department of Translational Medicine, University of Piemonte Orientale, Novara, Italy; [13]University of Freiburg, Signalling Research Centres BIOSS and CIBSS, Germany; [14]German Cancer Consortium (DKTK), PartnerSite Freiburg, Germany

Background & Aims: Despite recent translation of immunotherapies into clinical practice, the immunobiology of hepatocellular carcinoma (HCC), in particular the role and clinical relevance of exhausted and liver-resident T cells remain unclear. We therefore dissected the landscape of exhausted and resident T cell responses in the peripheral blood and tumor microenvironment of patients with HCC.

Methods: Lymphocytes were isolated from the blood, tumor and tumor-surrounding liver tissue of patients with HCC (n = 40, n = 10 treated with anti-PD-1 therapy). Phenotype, function and response to anti-PD-1 were analyzed by mass and flow cytometry ex vivo and in vitro, tissue residence was further assessed by immunohistochemistry and imaging mass cytometry. Gene signatures were analyzed in silico.

Results: We identified significant enrichment of heterogeneous populations of exhausted CD8+ T cells (TEX) in the tumor microenvironment. Strong enrichment of severely exhausted CD8 T cells expressing multiple immune checkpoints in addition to PD-1 was linked to poor progression-free and overall survival. In contrast, PD-1 was also expressed on a subset of more functional and metabolically active CD103+ tissue-resident memory T cells (TRM) that expressed few additional immune checkpoints and were associated with better survival. TEX enrichment was independent of BCLC stage, alpha-fetoprotein levels or age as a variable for progression-free survival in our cohort. These findings were in line with in silico gene signature analysis of HCC tumor transcriptomes from The Cancer Genome Atlas. A higher baseline TRM/TEX ratio was associated with disease control in anti-PD-1-treated patients.

Conclusion: Our data provide information on the role of peripheral and intratumoral TEX–TRM dynamics in determining outcomes in patients with HCC. The dynamics between exhausted and liver-resident T cells have implications for immune-based diagnostics, rational patient selection and monitoring during HCC immunotherapies.

Lay summary: The role of the immune response in hepatocellular carcinoma (HCC) remains unclear. T cells can mediate protection against tumor cells but are frequently dysfunctional and exhausted in cancer. We found that patients with a predominance of exhausted CD8+ T cells (TEX) had poor survival compared to patients with a predominance of tissue-resident memory T cells (TRM). This correlated with the molecular profile, metabolic and functional status of these cell populations. The enrichment of TEX was independently associated with prognosis in addition to disease stage, age and tumor markers. A high TRM proportion was also associated with better outcomes following checkpoint therapy. Thus, these T-cell populations are novel biomarkers with relevance in HCC.

Research Article   Hepatic and Biliary Cancer

Introduction

Hepatocellular carcinoma (HCC) represents a major global health problem. In patients with advanced disease, *i.e.* with portal invasion and extrahepatic spread but preserved liver function (Barcelona Clinic Liver Cancer [BCLC] stage C), prognosis is limited despite a growing number of systemic therapy options. Combination immunotherapy with anti-programmed cell death ligand 1 (PD-1) and anti-vascular endothelial growth factor antibodies has now become the first-line systemic therapy for advanced HCC, with an objective response rate of 29.8%.[1,2] Even though tumor antigen-specific responses have been shown to correlate with better survival in HCC,[3] only a fraction of ~20-25% of HCCs falls into an "immune class" with significant enrichment of immune signatures in the tumor.[4] This may explain the unsatisfactory results of phase III trials on anti-PD-1-based immune checkpoint monotherapy in HCC (nivolumab and pembrolizumab), with objective response rates of ~15-20%.[5,6]

Induction of exhausted CD8+ T cells (TEX) with reduced function is frequently implicated in cancer immune escape. TEX display major alterations of their differentiation program compared to functional effector and memory T cells.[7] They express multiple inhibitory receptors, such as PD-1 and cytotoxic T-lymphocyte antigen-4 (CTLA-4) that also serve as targets for immune checkpoint blockade (ICB). PD-1 is a key hallmark of T-cell exhaustion and was found to be enriched in T cells obtained from patients with HCC,[8–11] however, PD-1 can also be expressed by effector or memory T-cell populations, including tissue-resident memory T cells (TRM), that are implicated in protection. To fully characterize exhausted T cells, profiling of additional exhaustion features on a single-cell level is required to reveal the heterogeneity of exhausted T cells in chronic infections and cancer.[12] However, limited information is available about exhausted T-cell heterogeneity in HCC. Moreover, recent work in metabolic liver disease models points to a role of exhausted and resident immune cells regulated by PD-1 in driving HCC progression.[13,14]

In this study, we therefore aimed to understand the role and clinical associations of TEX and TRM in HCC. We performed in-depth phenotypic and functional exhaustion profiling of the peripheral and intrahepatic tumor T-cell compartments of patients with HCC using mass and flow cytometry as well as immunohistochemistry and imaging mass cytometry of tumor tissues. Single-cell- and population-based transcriptome profiles from published datasets of HCC resections were *in silico* assessed for signatures of T-cell exhaustion and their link to patient survival. The role of TRM and TEX in the response to anti-PD-1 checkpoint therapy was tested in a well-defined patient cohort and in *in vitro* experiments.

Our results show that the enrichment of TEX at the expense of TRM is linked to poor patient survival, in line with the functional and metabolic impairment observed for exhausted T cells. The expression of CD103, rather than C-X-C motif chemokine receptor 6 (CXCR6) and CD69, identified a non-exhausted TRM subset. A higher CD103+TRM/TEX ratio was associated with a better response to checkpoint therapy in patients. TEX populations displayed augmented function after anti-PD-1 blockade, indicating that both TRM and TEX contribute to the immune response during checkpoint therapy. These results point towards a delicate balance of CD103+ TRM and TEX in HCC

pathophysiology and implicate these immune populations as potential biomarkers and targets for personalized therapies.

Patients and methods

Patients

Samples from 30 patients with HCC, for whom peripheral blood mononuclear cells (PBMCs) and HCC biopsy or tumor resection tissue were available, and 5 healthy donors were recruited through the Hepatologic and Gastroenterologic biobank of the University Medical Center of Freiburg (HBUF) with written informed consent of all study participants and after approval by the Institutional Review Boards (Ethic Committee of the Albert-Ludwigs-University, Freiburg: 243/18, 474/14). Patients with radiologically or histologically confirmed HCC that had not received systemic therapy were included in this study. Table S1 summarizes the clinical data. Progression-free survival (PFS) was calculated as the number of days between successful therapeutic intervention closest to study enrollment and radiographic evidence of disease progression or time of death. Biopsy samples and clinicopathologic variables from an additional 10 patients with HCC undergoing subsequent anti-PD-1 checkpoint therapy were recruited from multiple centers as in[15] after approval by the local Institutional Review Boards. Inclusion criteria were i) Diagnosis of HCC by histopathology or imaging criteria according to AASLD and EASL guidelines; ii) systemic therapy with anti-PD-1 for HCC not amenable to curative or loco-regional therapy following local multidisciplinary tumor board review; iii) measurable disease according to RECIST v1.1 criteria at checkpoint therapy star; iv) Child-Pugh grade A. Disease staging by CT or MRI was conducted prior to and at approximately 9-weekly intervals during treatment.

Cell isolation

PBMCs were isolated from EDTA anticoagulated blood samples using Pancoll density gradient centrifugation. Intrahepatic lymphocytes from adjacent liver regions macroscopically non-infiltrated by the tumor (ATLs) and tumor-infiltrating lymphocytes (TILs) were isolated from HCC tissue by mechanical dissociation through a sterile 70 μM cell strainer (BD Biosciences, Franklin Lakes, NJ). Cells were freshly used or cryopreserved before staining.

Mass cytometry staining

Mass cytometry by time of flight (CyTOF) reagents were commercially obtained or generated by custom conjugation to isotope-loaded polymers using MAXPAR kit (Fluidigm). Mass cytometry panels used are shown in Table S2. Staining was performed as previously described.[12] Briefly, single-cell suspensions were pelleted, incubated with 20 μM Lanthanum-139-loaded maleimido-mono-amine-DOTA in PBS for 10 min at room temperature (RT) for live/dead discrimination. Cells were washed in staining buffer, resuspended in surface antibody cocktail, incubated for 30 min at RT, washed twice, pre-fixed with 1.6% PFA, washed, then fixed and permeabilized using FoxP3 kit, and stained intracellularly for 60 min at RT. Cells were further washed twice before fixation in 1.6% PFA (Electron Microscopy Sciences) solution containing 125 nM Iridium overnight at 4°C. Prior to data acquisition on a CyTOF Helios (Fluidigm), cells were washed twice in PBS and once in dH2O. The antibodies

used for mass cytometry and flow cytometry are listed in the CTAT table.

Statistical analysis

Statistical analyses were performed using GraphPad Prism V.8 (GraphPad Prism Software, USA) and R studio (R studio, USA). Bar charts show mean values with SD, statistical tests used are depicted in the figure legends. Correlation analyses were performed for continuous *vs.* continuous parameters using Spearman rank correlation, for continuous *vs.* binary variables using unpaired Wilcoxon test and for binary *vs.* binary variables using Fisher's exact test. Further details on correlation analysis and the cox proportional hazard models used are provided in the supplementary data. Levels of significance are indicated as follows: *p <0.05; **p <0.01; ***p <0.001.

Results

Heterogeneous CD8 T-cell exhaustion profiles in HCC patients

We comprehensively profiled the peripheral and intrahepatic immune compartments of patients with HCC (Fig. 1A). Key immune lineages were analyzed in PBMCs, ATLs and TILs using highly multiplexed mass cytometry (Fig. 1B) (Table S2). We focused on the analysis of CD8 T cells using a comprehensive panel of exhaustion-related immune checkpoints PD-1, LAG-3, CTLA-4, KLRG1, Tim-3 and TIGIT, ectoenzymes CD38 and CD39, transcription factors Eomes, Helios, Tcf-1, T-bet and Tox, in addition to other markers of T-cell differentiation and function. These markers allow for the differentiation of several distinct TEX subsets.[12,16] Clearly, the CD8 T-cell landscape visualized by t-distributed stochastic neighbor embedding (t-SNE) analysis differed between the peripheral blood, non-tumor liver and tumor tissue (Fig. 1C).

To understand these differences in the CD8 T-cell landscape, we first assessed the exhaustion marker profile between the immune compartments (Fig. 1D). While this data confirmed expected differences between the peripheral blood (which was enriched for naïve and memory populations of CD8 T cells expressing CCR7, CD27, CD28, CD73, CD127) and the tumor (lacked naïve and central memory populations), they also revealed differences between the samples obtained from the tumor or adjacent liver (Fig. 1D). PD-1 and other exhaustion markers, such as CD39, CTLA-4, TIGIT, Tox or Eomes were expressed by CD8 T cells isolated from the tumor tissue, however, only ~1/3 of patients displayed high co-expression of PD-1, Eomes, CD160 and CD39, providing information on severe exhaustion phenotypes. The expression of these markers was lower in other patient TILs, in which reduced levels of Eomes but higher levels of tissue-residency marker integrin αE (CD103) were observed, indicating CD8 T-cell heterogeneity in TILs from patients with HCC (Fig. 1D). Despite this heterogeneity, we observed the highest expression of exhaustion markers PD-1 and CD39 in TILs, with some expression in ATLs (Fig. 1D, E). Similarly, the inhibitory receptor LAG-3 was upregulated in the TIL and ATL compartments, while transcription factor Tcf-1 was reduced. These results are in line with an accumulation of exhausted T cells in the HCC tumor microenvironment.

Strong PD-1 TIL enrichment is associated with poor PFS and overall survival

The marked heterogeneity of PD-1 expression observed between patients prompted us to test if differential PD-1 expression could also provide information about patient outcomes, which was predicted based on studies focusing on PD-1 expression but using a limited set of exhaustion markers in HBV-associated HCC.[11,17] We first discriminated patient groups based on their peripheral and intrahepatic CD8 T-cell PD-1 expression levels, an analysis which did not show an association with outcome (Fig. 1F). We reasoned that the dynamics between the peripheral and intrahepatic compartment, such as accumulation of recirculating T cells, might be better reflected by the enrichment in the tumor and thus assessed the ratio of PD-1 expressing T cells between the peripheral blood and the tumor tissue. This analysis revealed a clear link between strong enrichment of PD-1-positive CD8 T cells in the tumor with poor PFS and overall survival (OS) (Fig. 1G). These data implicate the accumulation of exhausted T cells in detrimental HCC outcomes. However, the heterogeneity of PD1-expressing CD8 T-cell phenotypes observed here and the absence of a direct correlation of intrahepatic PD-1-expressing T cells with outcome indicated that not all PD-1-expressing CD8 T cells are associated with an exhaustion phenotype and detrimental outcomes.

Exhaustion genes associated with poor progression in The Cancer Genome Atlas HCC dataset

To test if epigenomic exhaustion genes are also able to discriminate outcomes in bulk tumor transcriptome data, we assessed the genes within the epigenomic exhausted signature[12] in the liver cancer data obtained from The Cancer Genome Atlas database.[18] Indeed, a linear predictor based on weighted exhaustion genes discriminated patient survival, with the higher exhaustion predictor associated with worse survival (Fig. S2A). While these data fit to our experimental observations (Fig. 1), we also noted that several exhaustion genes were individually also associated with better survival (*i.e.* Gzmk, Eomes), and an unweighted exhaustion analysis did not discriminate patient outcomes *per se* (Fig. S2B,C), suggesting differential roles for different exhaustion genes or additional heterogeneity of exhausted T cells not explained on this bulk analytical level.

A higher TRM fraction of CD8+ PD-1+ T cells in tumor tissue is linked to better survival

To further understand the PD-1 enrichment association with patient outcomes, we next focused on the roles of different T cell populations that can express PD-1. These include TRM, which can be identified by CD103 expression and typically co-express CD69 and CXCR6.[19] Analysis of PD-1 and CD103 on the CD8 t-SNE map (Fig. 1C) pointed to different populations of PD-1 and CD103 co-expressing cells (Fig. 2A). The t-SNE fingerprint of PD-1 strong enricher patients as identified in Fig. 1 suggested reduced CD103 expression (Fig. 2A). We therefore dissected TRM phenotypes in our cohort. As expected, TRM were enriched in the liver (ATLs and TILs) compared to the blood, where CD103+ T cells were practically absent (Fig. 2B). Of note, in ATLs and TILs, a mean of 37% and 42% of TRM expressed PD-1 in the ATL and TIL compartments, respectively (Fig. 2B). The fraction of CD103+ cells among the PD-1+ population varied widely, with a mean of 30% in TILs (Fig. 2B). In addition, we performed *in silico* analysis of single-cell RNA-sequencing data in a previously published HCC dataset of 686 CD8+ T cells[20] and found comparable distributions of these PD-1+ and CD103+ T-cell populations in TILs (Fig. S3).
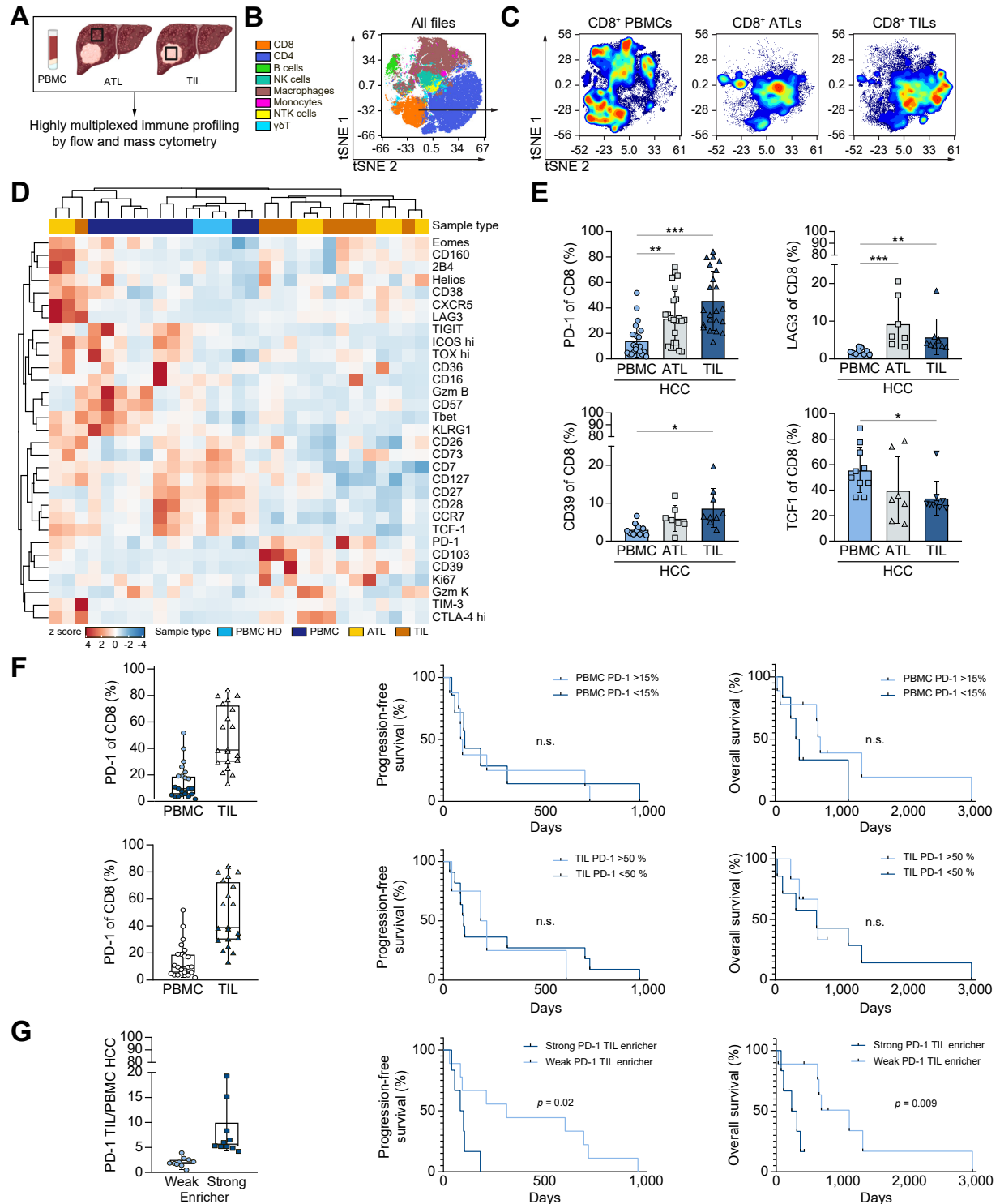
Fig. 1. Immune profiling of CD8+ T cells in HCC. (A) Study workflow. Blood and tumor and adjacent tumor tissue samples from patients with HCC (n = 40) were analyzed. (B) t-SNE representation of HCC immune compartments and distribution of key immune lineages. (C) t-SNE of CD8+ T-cell immune compartments subdivided by origin. (D) Hierarchically clustered heatmap of T-cell phenotype showing marker expression (percent of CD8+) is represented by z-scores after column normalization. (E) Frequency of PD-1, LAG-3, CD39 and TCF1 on CD8+ PBMCs, ATLs and TILs. (F) Kaplan-Meier analysis of PFS and OS based on high peripheral and TIL PD-1 expression levels (threshold: 15%, 50% respectively). (G) PD-1 TIL enrichment was stratified based on PD-1+ TIL/PD-1+ PBMC quotient. PFS and OS analysis of PD-1 TIL strong and weak enrichers are shown. Tick marks indicate censored data in F and G. Data represent means ± SD, Kruskal-Wallis test was used in D. Log-rank test was used for survival analysis. *p <0.05, **p <0.01, ***p <0.001. ATLs, adjacent non-tumor tissue lymphocyte(s); HCC, hepatocellular carcinoma; OS, overall survival; PBMCs, peripheral blood mononuclear cells; PFS, progression-free survival; TILs, tumor-infiltrating lymphocytes; t-SNE, t-distributed stochastic neighbor embedding.
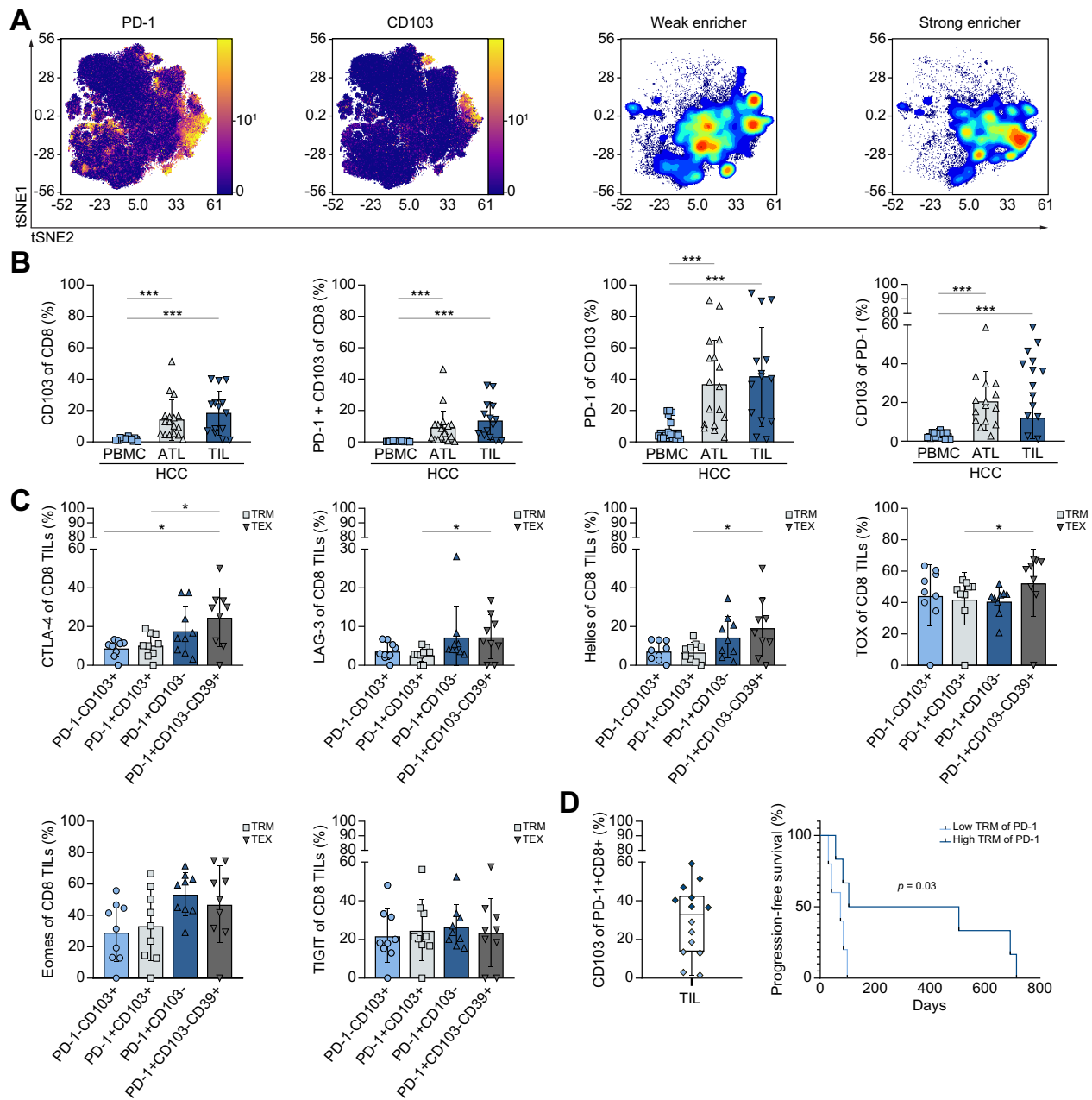
Fig. 2. CD103+ TRM cells associate with better outcome in HCC. (A) (left) PD-1 and CD103 expression is indicated on the t-SNE map as in Fig. 1C (right) CD8 T-cell distribution stratified based on PD-1 TIL enrichment. (B) Analysis of the frequencies of CD103 and PD-1 CD8 subpopulations. (C) Expression analysis of exhaustion-related markers CTLA-4, LAG-3, Helios, Tox, Eomes, and TIGIT between TRM (PD-1-CD103+ and PD-1+CD103+) and TEX (PD-1+CD103- and PD-1+CD103-CD39+) CD8+ subsets. (D) Survival analysis of patients with high TRM fraction of PD-1+ CD8+ TILs in comparison to patients with low TRM fraction. Data indicate means ± SD, Kruskal-Wallis test was used in B, Mann-Whitney *U* test was used for comparison of TRM and TEX in C. Log-rank test was used for survival analysis. *p <0.05, **p <0.01, ***p <0.001. ATLs, adjacent non-tumor tissue lymphocyte(s); HCC, hepatocellular carcinoma; PBMCs, peripheral blood mononuclear cells; TEX, exhausted CD8+ T cells; TILs, tumor-infiltrating lymphocytes; TRM, tissue-resident memory T cells; t-SNE, t-distributed stochastic neighbor embedding.

Severe T-cell exhaustion is associated with co-expression of multiple inhibitory receptors and a specific transcriptional program.[21,22] We thus tested for the co-expression of several exhaustion markers on PD-1-CD103+ and PD-1+CD103+ TRM, PD-1+CD103- cells and the severe exhausted phenotype (PD-1+CD103-CD39+ TEX). There was no significant difference between PD-1-CD103+ and PD-1+CD103+ TRM cells with respect to expression of other exhaustion markers. Notably, TEX expressed significantly higher levels of inhibitory receptors CTLA-4 and LAG-3 as well as transcription factors Helios and Tox compared

to TRM (Fig. 2C). These results indicate that PD-1+TRM co-express fewer immune checkpoints than TEX. We next wondered if the differential contribution of TRM to the PD-1+ T-cell pool was associated with patient outcome. Indeed, higher fractions of TRM in the PD-1+ T-cell pool were associated with significantly better PFS (Fig. 2D). Together, these results illustrate that distinct PD-1-expressing T-cell subsets are differentially linked to patient outcome.

Absence of CD4+ TRM but enrichment of PD-1+ regulatory T cells and T follicular regulatory cells in HCC tumor tissue

We next asked if the role for TRM observed for CD8+ T cells would also apply to CD4+ T cells. The CD4+ T-cell landscape differed largely between PBMCs, ATLs and TILs (Fig. 3A). While there was also a trend towards higher PD-1 expression on CD4+ T cells in TILs, CD103+ TRM were virtually absent or present in only very low numbers (mean <1% of TIL CD4), in contrast to the results observed with CD8+ T cells (Fig. 3B).

Nevertheless, we observed an upregulation of CD39, CTLA-4 and LAG-3 in CD4+ TILs and a reduction in Tcf-1 expression (Fig. 3C). Of note, the expression of these markers was due to the enrichment of regulatory T cells and T follicular regulatory T cells (Tfr) rather than a CD4 exhaustion or residency phenotype (Fig. 3D). In sum, our analysis suggests the relative absence of a CD103+ TRM population within the CD4+ compared to the CD8+ T cell pool.
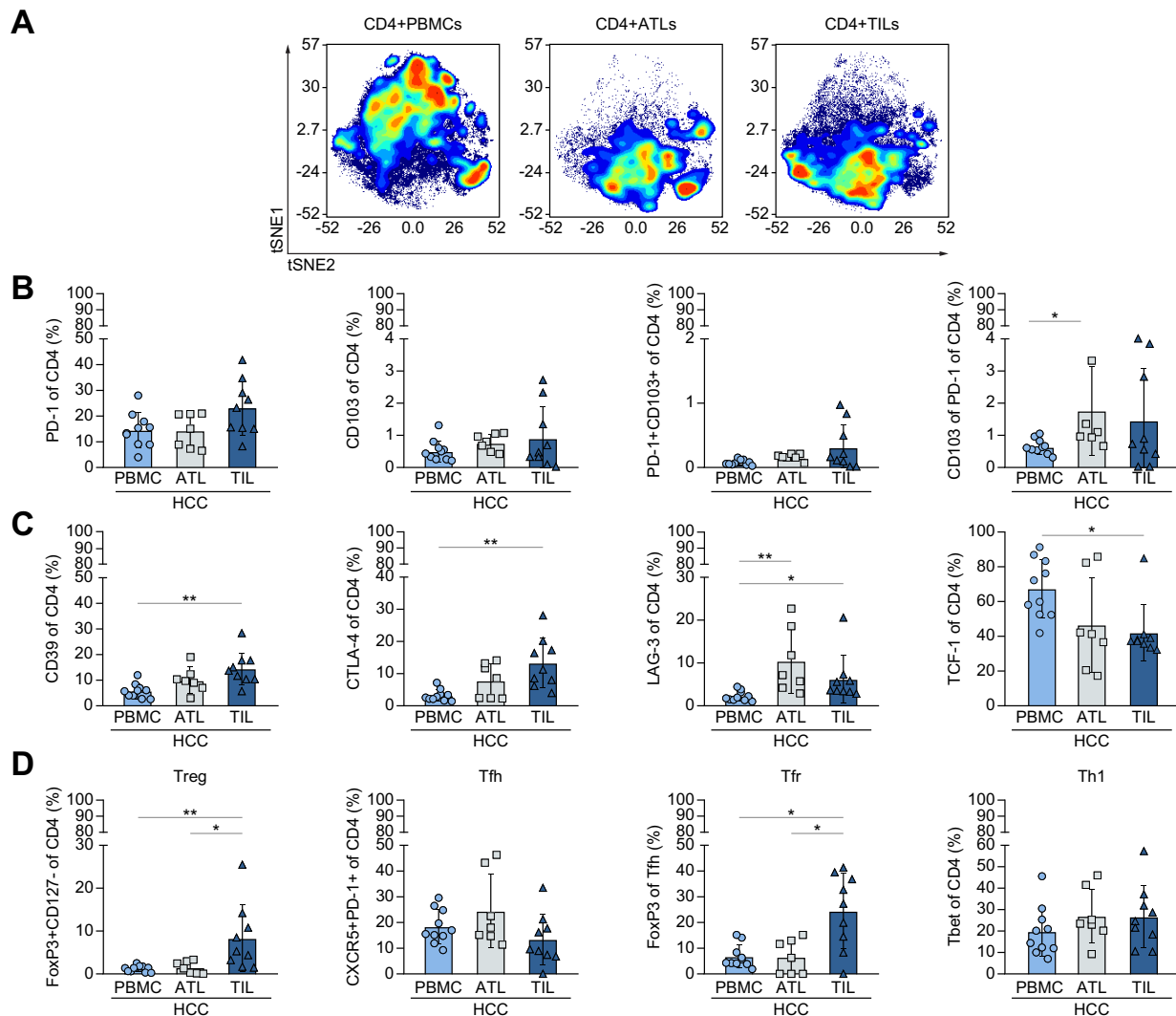

Fig. 3. **Enrichment of Treg, Tfh and Tfr populations, but absence of CD103+ CD4+ TRM in HCC.** (A) t-SNE visualization of the CD4 landscape in PBMCs, ATLs and TILs. (B) Frequency of indicated PD-1 and CD103 expressing subsets. (C) Expression of CD39, CTLA-4, LAG-3 and TCF-1 in CD4+ T cells across between the immune compartments. (D) Analysis of Treg (FoxP3+CD127-), Tfh (CXCR5+PD-1+), Tfr (FoxP3+ of Tfh) and Tbet+Th1 CD4+ T cells between PBMCs, ATLs and TILs. Data represent means ± SD, Kruskal-Wallis test was used in B-D. *p <0.05, **p <0.01. ATLs, adjacent non-tumor tissue lymphocyte(s); HCC, hepatocellular carcinoma; PBMCs, peripheral blood mononuclear cells; Tfh, T follicular helper cells; Tfr, T follicular regulatory cells; TILs, tumor-infiltrating lymphocytes; Treg, regulatory T cells; t-SNE, t-distributed stochastic neighbor embedding.
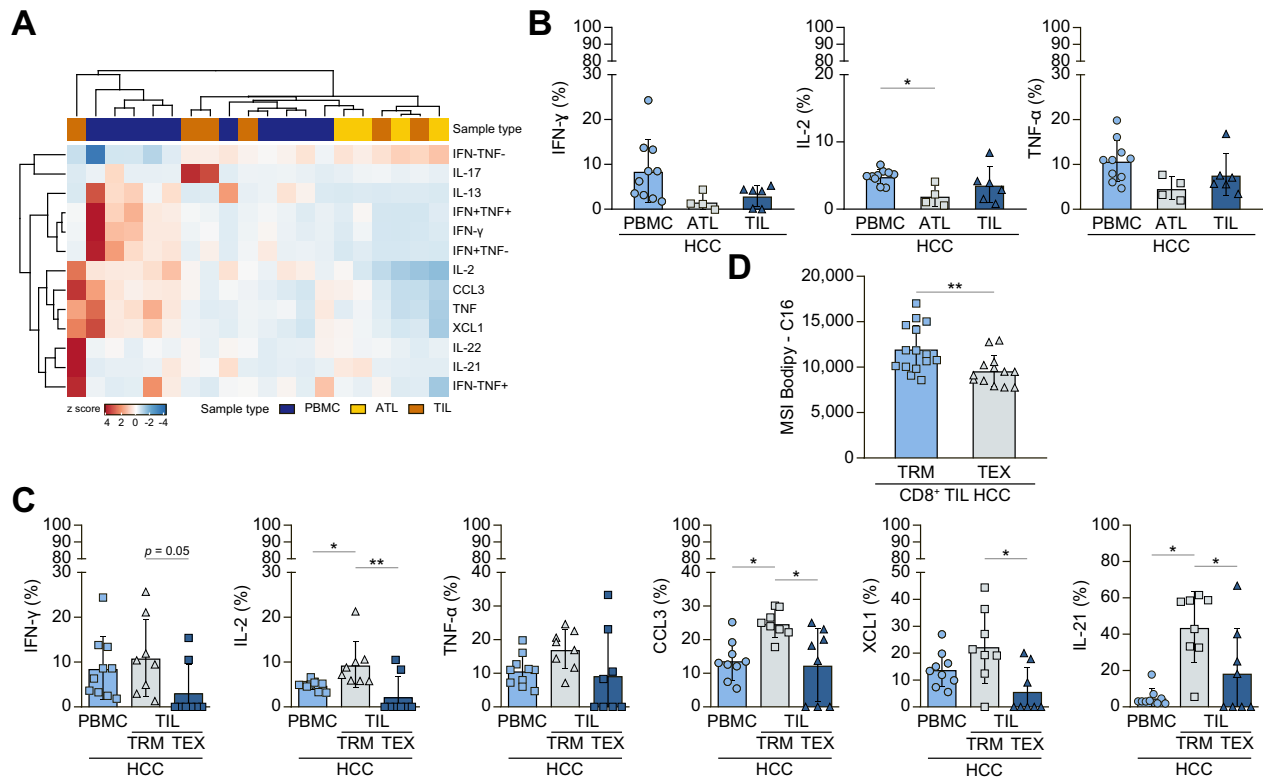
Fig. 4. Enhanced T-cell function and lipid uptake of CD103+ TRM in HCC. (A) Hierarchically clustered heatmap of CD8+ T-cell function showing percentages of cytokine and chemokine marker expression after PMA/Ionomycin stimulation. (B) Bulk CD8 T-cell IFN-γ, IL-2 and TNF-α production is compared between PBMCs, ATLs and TILs. (C) Comparison of IFN-γ, IL-2, TNF-α, CCL3, XCL1 and IL-21 production between CD8+ PBMCs, and TRM (PD-1+CD69+CD8+) and TEX (PD-1+CD69-CD39+CD8+) in the TIL compartment. (D) Bodipy-C16 uptake was compared between TEX and TRM. Data represent means ± SD, Kruskal-Wallis test (B-C), Mann-Whitney U test (D). *p <0.05, **p <0.01, ***p <0.001. ATLs, adjacent non-tumor tissue lymphocyte(s); HCC, hepatocellular carcinoma; PBMCs, peripheral blood mononuclear cells; TEX, exhausted CD8+ T cells; TIL, tumor-infiltrating lymphocyte; TRM, tissue-resident memory T cells.

Superior function and metabolic activity of CD8+ TRM

To explore cellular correlates of the protective function of TRM over TEX within the PD-1+ T cell pool, we assessed the poly-functionality profile of T cells after stimulation (Table S2). These analyses revealed distinct functional profiles between PBMCs, ATLs and TILs (Fig. 4A), with some reduction in T cell functionality in the liver (Fig. 4B). We specifically examined the cytokine and chemokine production of TEX and compared it with peripheral and TRM cells. Clearly, TEX displayed a lower production of interferon-γ (IFN-γ), interleukin (IL)-2, IL-21, C-C motif chemokine ligand 3 (CCL3) and X-C motif ligand 1 (XCL1) than TRM (Fig. 4C). These data demonstrate superior T cell functionality associated with the protective role of TRM in contrast to TEX.

Mechanistically, reduced metabolic activity has been linked to the dysfunction of TEX.[22] In contrast, a preference of resident CD8+ T cells towards exogenous free fatty acids was described in the skin.[23] We thus analyzed the uptake of exogenous free fatty acids using C16-Bodipy reagent. We found that TRM exhibited stronger fatty acid uptake compared to TEX (Fig. 4D). These results fit to the notion of higher metabolic fitness of TRM as a prerequisite for protective immunity.

Expression of CD103, but not CXCR6, identifies non-exhausted TRM

In addition to CD103, chemokine receptor CXCR6 and CD69 are markers associated with hepatic tissue residency but their individual roles in HCC remain unclear. We thus dissected the TRM landscape by co-analyzing exhaustion and tissue residency markers in an additional cohort of patients with HCC. As shown in Fig. 5A, CD103, CXCR6 and CD69 were all enriched in TILs compared to PBMCs, as expected, however CD103 was expressed by markedly less CD8 TILs compared to CD69 and CXCR6. Clearly, CD103+ TRM co-expressed high levels of CD69 and CXCR6 (Fig. 5B), however, CXCR6 and CD69 expression was also found on cells with a more exhausted phenotype (Fig. 5CD). In contrast, the CD103+ TRM population did not express significant levels of Eomes or Tox, key transcription factors associated with the exhaustion program, as well as lower levels of exhaustion-associated checkpoints CD38, CD39, TIGIT and CTLA-4 (Fig. 5C). Notably, we also observed a significantly higher pro-inflammatory polyfunctionality of CD103+ TRM compared to CXCR6+ and CD69+ T cells that did not express CD103, or TEX, upon stimulation (Fig. 5E). These analyses indicate that CD103
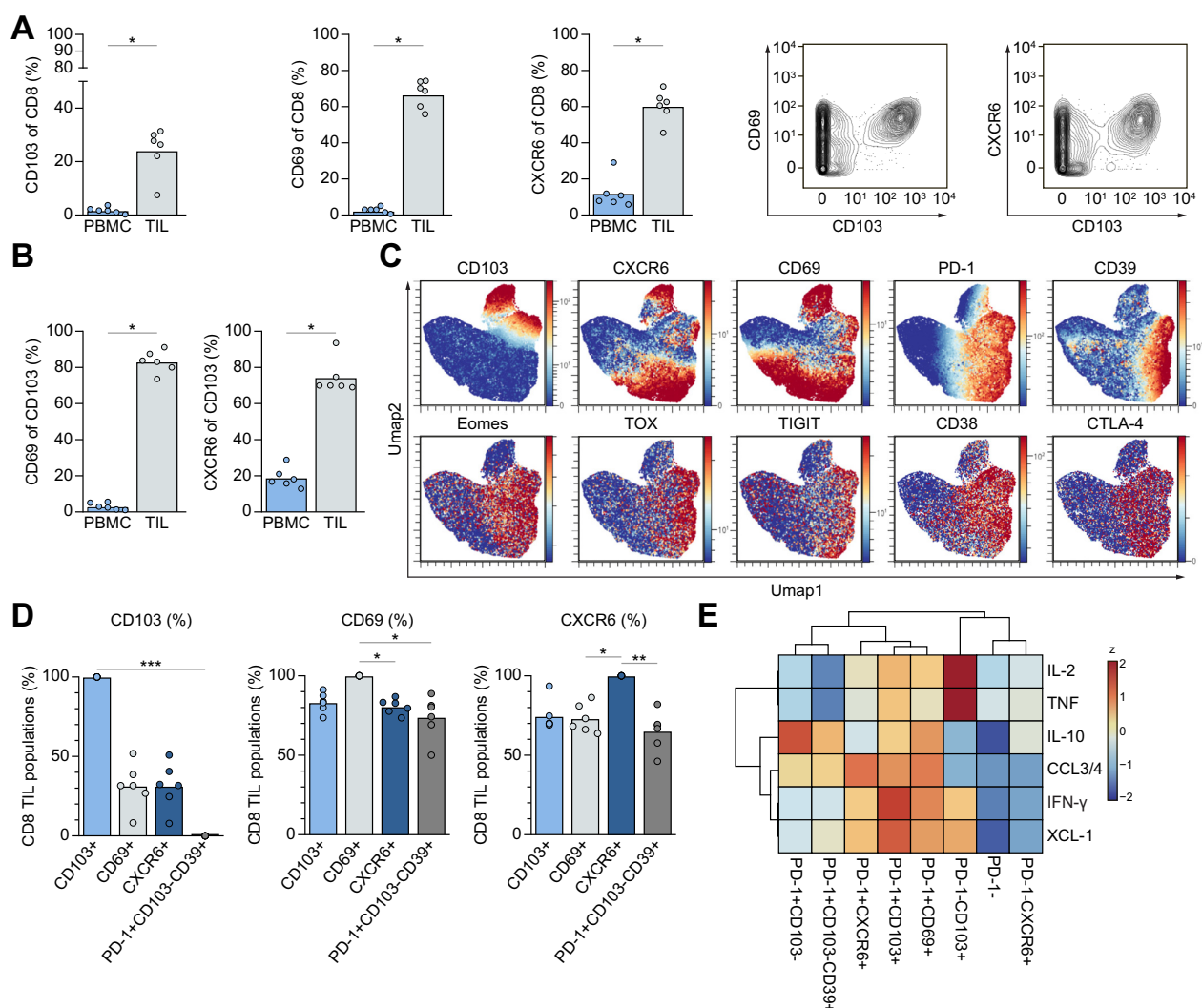
Fig. 5. Phenotypic and functional characterization of the TRM landscape in HCC identifies a non-exhausted CD103+ TRM population. (A) Analysis of TRM markers CD103, CD69 and CXCR6 between PBMCs and TILs and exemplary contour plots in HCC TILs gated on live CD8 T cells. (B) Expression of CD69 and CXCR6 was assessed on CD103+CD8+ T cells. (C) UMAP and visualization of residency (CD103, CXCR6, CD69) and exhaustion (PD-1, CD39, Eomes, Tox, TIGIT, CD38, CTLA-4) markers in CD8 TILs. (D) Frequency of CD103, CD69 and CXCR6 assessed on CD103+, CD69+, CXCR6+, PD-1+CD103-CD39+ (TEX) CD8 TIL populations. (E) Hierarchically clustered heatmap of TRM and TEX CD8 TIL populations indicating percentages of cytokine expression visualized by z-score based coloring (column normalization). Wilcoxon test was used in A, B, D. $^*p$ <0.05, $^{**}p$ <0.01, $^{***}p$ <0.001. HCC, hepatocellular carcinoma; PBMCs, peripheral blood mononuclear cells; TEX, exhausted CD8+ T cells; TILs, tumor-infiltrating lymphocytes; TRM, tissue-resident memory T cells; UMAP, uniform manifold approximation and projection.

expression, more specifically than CXCR6 or CD69 expression, identifies functionally competent TRM populations in HCC.

PD-1+CD103+ TRM engage closely with tumor cells
Next, we addressed the spatial relationship of TRM and TEX in HCC tissue. First, immunohistochemical staining of HCC tissue was performed, including CD8, PD-1 and CD103, with double labeling of CD8 and PD-1 in corresponding adjacent sections (Fig. 6A). This staining showed the presence of CD103+PD-1+ T cells within lymphoid aggregates and also infiltrating the tumor (Fig. 6A). To overcome the limitations of immunohistochemistry that only allow for co-analysis of a few markers, we performed highly multiplexed imaging mass cytometry of HCC tissues that provided a detailed assessment of TRM and TEX markers by co-

expression analysis at a single-cell level. As shown in Fig. 6B and Fig. S4, PD-1+CD103+ TRM CD8+ T cells could be identified with relatively high T-cell density and in close engagement with tumor cells in some patients with longer PFS. In contrast, PD-1+CD103- TEX CD8+ T cells were frequently identified in tumors from patients with a relative paucity of an immune infiltrate and lower PFS. In sum, these data highlight that PD-1+CD103+ TRM infiltrate HCC tumors as a likely correlate of their protective function.

Multivariate analysis validated strong PD-1 enrichment to be an independent predictor of reduced PFS in patients with HCC
We correlated our immunological findings with relevant clinical parameters, such as BCLC tumor stage, alpha-fetoprotein (AFP)
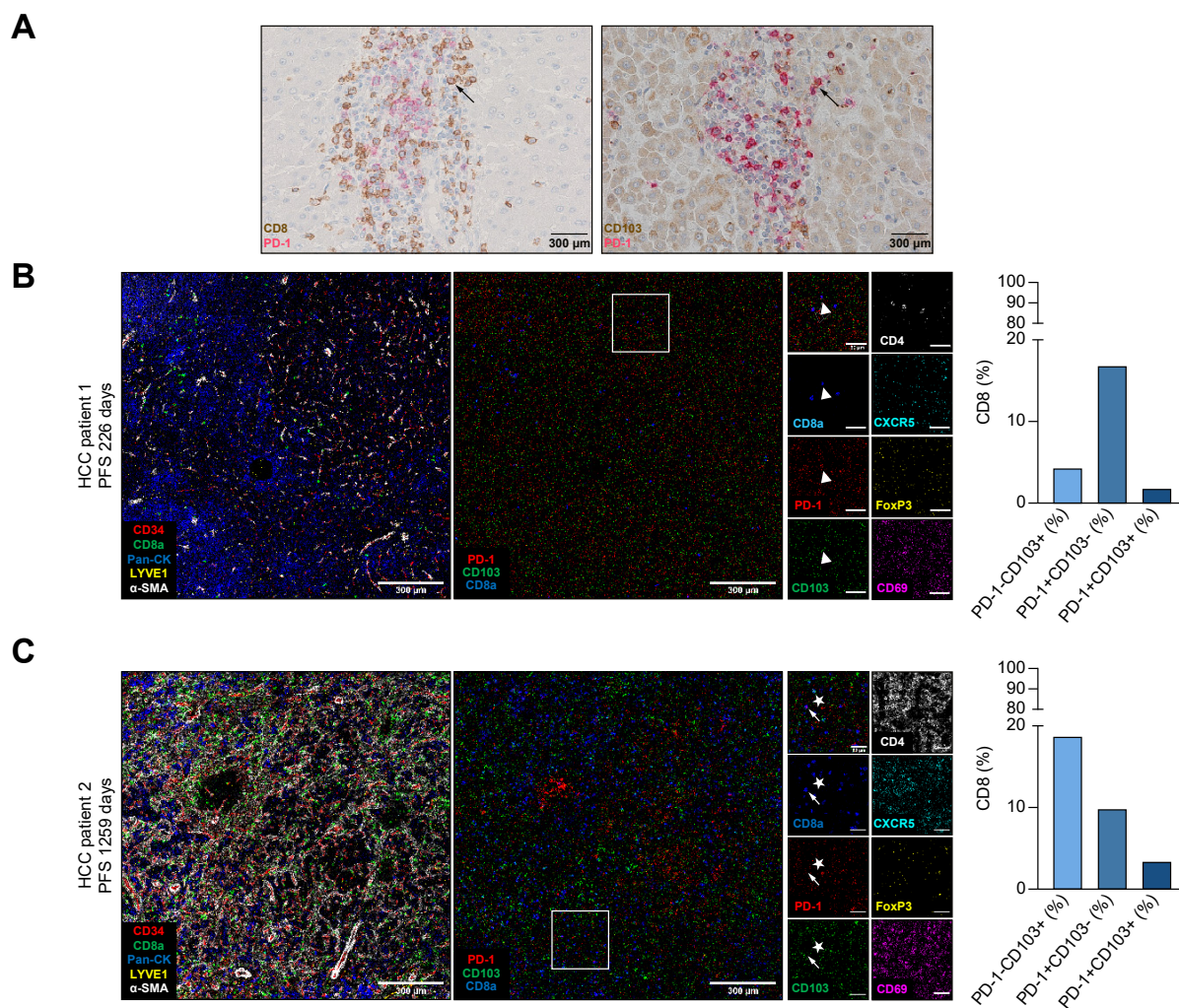
Fig. 6. Immunohistochemistry and imaging mass cytometry of HCC tissue. (A) Exemplary immunohistochemistry of HCC tissue stained for CD8 (brown), PD-1 (red) and CD103 (brown) (40x, scale bar: 300 μm). Left arrows indicate co-staining of CD8 and PD-1 (red-brown), right arrows indicate co-expression of PD-1 and CD103 (red-brown) in corresponding tumor sections. (B) Pseudocolored imaging mass cytometry images of HCC tissue from 2 exemplary HCC patients with short (patient 1) and long PFS (patient 2): CD8 (green), CD34 (red), pan-CK (blue) LYVE1 (yellow) and α-SMA (white) in images on the left and PD-1 (red), CD103 (green), CD8 (blue), CD4 (white), CXCR5 (light blue), FoxP3 (yellow) and CD69 (pink) in the overview image on the right and inserts. Triangles point to PD-1+CD103-CD8+ T cells (patient 1), arrows to PD-1+CD103+CD8+ T cells and the asterisks to PD-1-CD103+CD8+ T cells (patient 2). Bar graphs show frequency of PD-1-CD103+, PD-1+CD103-, and PD-1+CD103+ CD8 T-cell populations. Scale bar indicates 300 μm in the overview images and 50 μm in the inserts. HCC, hepatocellular carcinoma; PFS, progression-free survival.

level, etiology, and PFS (Fig. 7). Enrichment of exhausted T cells correlated positively with AFP levels and BCLC B and C stage, while it was negatively correlated with earlier disease stages, pointing to a role of exhausted T cells in HCC progression. In contrast, earlier disease stages showed a positive correlation with PD-1+CD103+ TRM frequencies. The strongest correlation of TEX enrichment with disease etiology was found for non-alcoholic steatohepatitis (NASH)-derived HCCs (Fig. 7).

To evaluate if PD-1 enrichment is an independent predictor of PFS, we performed multivariate analysis using a cox proportional hazards model with independent comparison of different variables (age, AFP, BCLC stages and PD-1 enrichment). Strong PD-1 enrichment was an independent predictor of decreased PFS in patients with HCC ($p = 0.03$) (Table S3). In sum, these analyses

highlight the intrahepatic enrichment of exhausted T cells as a useful biomarker for HCC.

Higher TRM/TEX ratio is associated with disease control in anti-PD-1-treated patients with HCC

It remained unclear if the TRM and TEX balance also played a role in patients treated with anti-PD-1 checkpoint therapy, which could target both TRM and TEX cells. We thus performed imaging mass cytometry analysis and single-cell level segmentation on samples from a well-defined clinical cohort of patients with unresectable/advanced HCC and compensated liver function (Child-Pugh A)[15] with tumor samples obtained prior to anti-PD-1 checkpoint therapy (Fig. 8A). Interestingly, patients with disease progression had less abundant CD8 T cells, suggesting
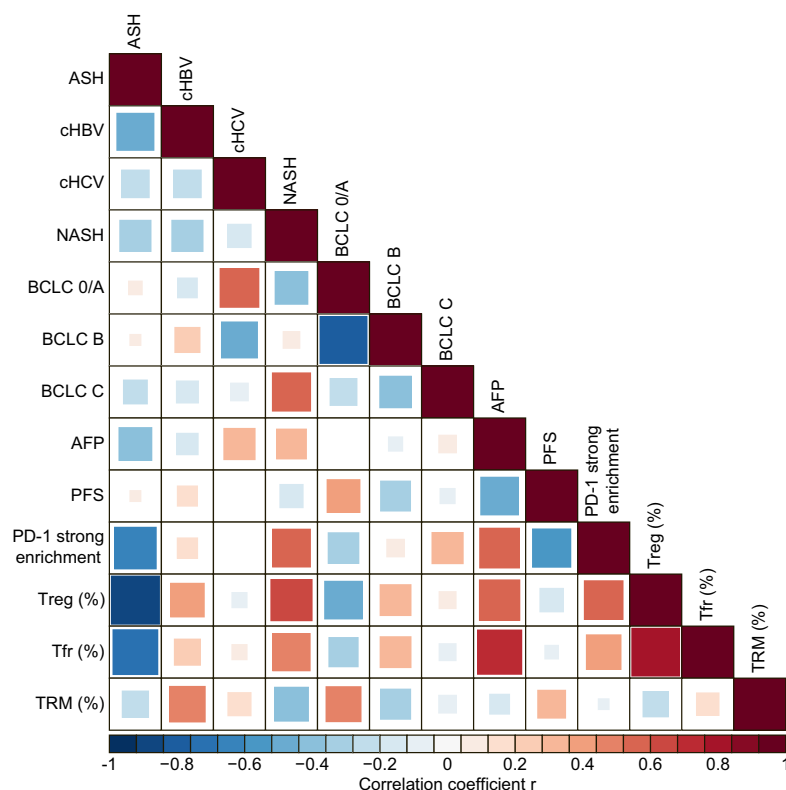
A

Fig. 7. Correlation of immunological and clinical parameters. T-cell subsets of interest were correlated with clinical parameters in a non-parametric correlation matrix. TRM were defined as PD-1+CD103+ CD8+ TILs, Treg as FoxP3+CD127-CD4+ and Tfr as FoxP3+CXCR5+PD-1+CD4+ TILs. Statistical tests: 1. Continuous *vs.* continuous parameters using Spearman rank correlation. 2. Continuous *vs.* binary variables using unpaired Wilcoxon test. 3. Fisher's exact test for testing of binary *vs.* binary variables. Positive correlations are indicated in red, negative correlations in blue, as indicated by the heatmap color bar. Both color and size of squares represent the Spearman correlation coefficient. AFP, alpha-fetoprotein; ASH, Alcoholic steatohepatitis; BCLC, Barcelona Clinic Liver Cancer; cHBV, chronic hepatitis B virus infection; cHCV, chronic hepatitis C virus infection; NASH, non-alcoholic steatohepatitis; PFS, progression-free survival; Tfr, T follicular regulatory cells; TILs, tumor-infiltrating lymphocytes; Treg, regulatory T cells; TRM, tissue-resident memory T cells.

that T cell presence is required for disease control during checkpoint therapy (Fig. 8B). We noted a higher abundance of both TEX and CD103+ TRM in patients with stable disease (Fig. 8B, C). Interestingly, the TRM/TEX ratio was positively correlated with a longer OS (Fig. 8D). These data suggested that a higher fraction of CD103+ TRM contributes to better outcomes during checkpoint therapy.

Anti-PD-1 checkpoint therapy *in vitro* augments TEX function
It remained unclear if the association of the TRM/TEX ratio with survival was due to direct augmentation of cellular function in response to anti-PD-1 antibodies. We therefore tested the response of TEX and TRM isolated from HCC tumors to anti-PD-1 checkpoint therapy in short-term cultures *in vitro* (Fig. 8E). Anti-PD-1 treatment resulted in slightly increased CD8 T cell numbers, and higher expression of cytokines IFN-γ, CCL3/4 and IL-2, indicating better T-cell effector function (Fig. 8F, G). There was no significant change in CD103+ TRM populations, however, we observed an expansion of PD-1+CD103-CD39+ TEX cells upon anti-PD-1 therapy (Fig. 8H). In line with our previous findings, CD103+ TRM had a higher cytokine production compared to TEX in the absence of anti-PD1 therapy, however, in this assay, TRM function was not significantly changed after checkpoint therapy independent of their PD-1 expression (Fig. 8I). In contrast,

CD103-TEX produced significantly more effector cytokine IFN-γ after checkpoint therapy, resulting in a similar level of effector function as TRM (Fig. 8I). In sum, these *in vitro* data indicate that anti-PD-1 therapy preferentially reinvigorates TEX to a level comparable to CD103+ TRM subsets. Taken together, these data indicate that a higher fraction of TRM over TEX is beneficial for patient outcomes, with anti-PD-1 augmenting the function of TEX populations, suggesting that both TRM and TEX contribute to anti-tumor immunity during HCC checkpoint therapy.

Discussion
With the advent of immunotherapies in HCC, a better understanding of the underlying immune populations is of crucial importance. Herein, we dissected the role of CD8 T-cell populations expressing major checkpoint receptors that can be targeted by immunotherapies using deep immunophenotyping by mass cytometry, imaging mass cytometry and *in silico* transcriptome analysis of patients with HCC. We found that PD-1 is expressed in the liver and tumor tissue by two major CD8+ T-cell populations that display significant differences in function and are associated with opposing clinical outcomes: (i) exhausted T cells with limited functionality and poor protective capacity and (ii) CD103+ resident memory T cells with higher effector function, metabolic activity and positive association with outcome.
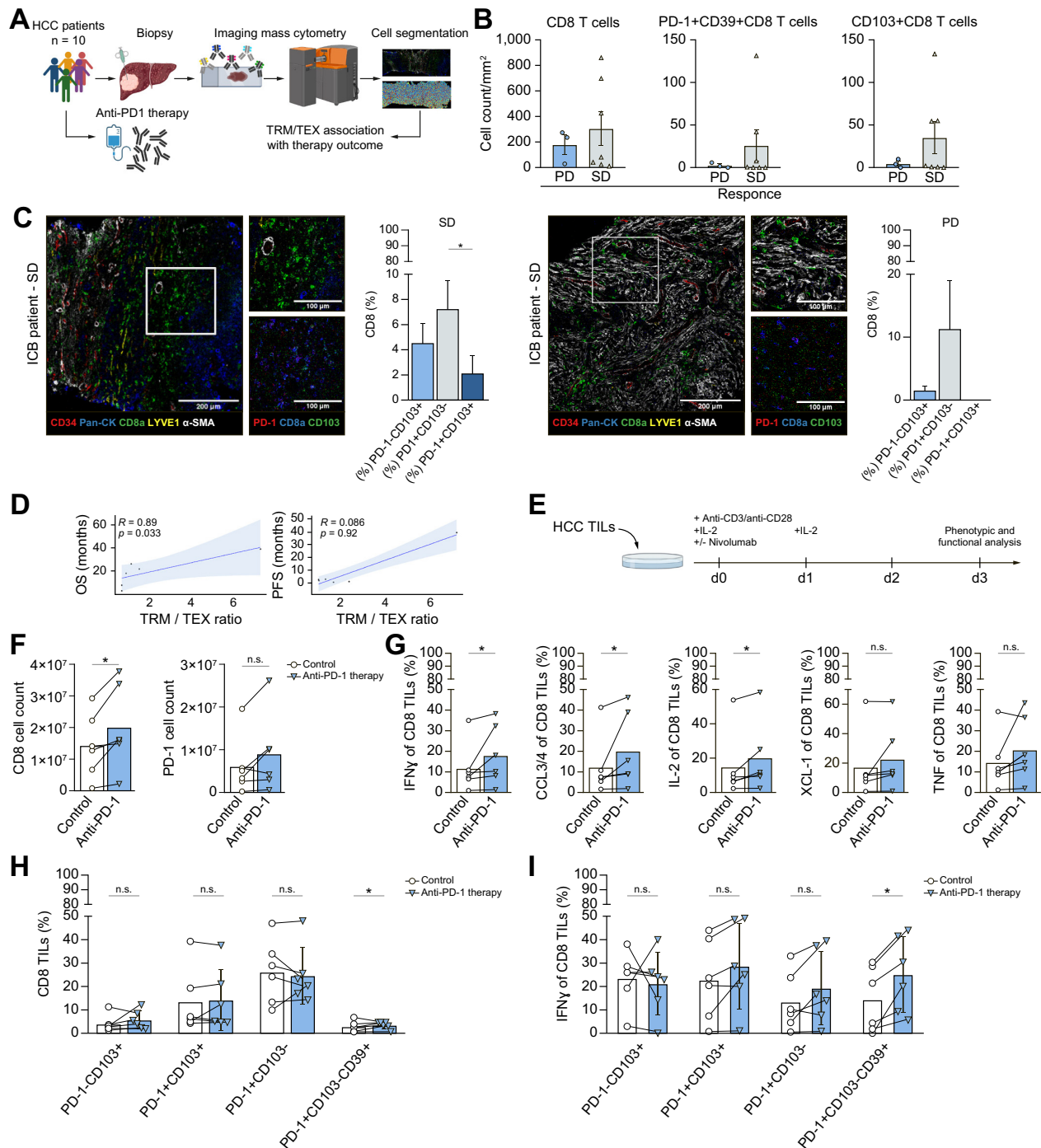
Fig. 8. Role of TRM and TEX cells for anti-PD-1 checkpoint therapy. (A) Overview of the experimental workflow. Liver biopsies from 10 patients with HCC starting anti-PD1 monotherapy were analyzed by imaging mass cytometry. (B) Bar graphs comparing cell counts of CD8 T cells, PD-1+ CD39+ CD8 T cells (TEX) and CD103+ CD8 T cells (TRM) per mm^2 HCC tissue between patients with PD and SD. (C) Pseudocolored imaging mass cytometry images of HCC tissues from 2 different patients with SD and with PD: CD8 (green), CD34 (red), pan-CK (blue) LYVE1 (yellow) and α-SMA (white) in the left images and upper inserts and PD-1 (red), CD103 (green) and CD8 (blue) in the lower inserts. Bar graphs show frequency of PD-1-CD103+, PD-1+ CD103- and PD-1+CD103+ of total CD8+ T cells. Scale bar indicates 200 μm (left images) or 100 μm (inserts). (D) Spearman correlation of TRM/TEX ratio with OS and PFS of checkpoint therapy study patients. (E) Workflow of the *in vitro* PD-1 blockade experiment after T-cell stimulation with anti-CD3/anti-CD28, IL-2 and +/- anti-PD-1 (nivolumab). Phenotypic and functional analysis was performed on d3 after restimulation with PMA/Ionomycin. (F) CD8 and CD8+PD-1+ cell count at d3 between control and anti-PD-1 group. (G) Analysis of IFN-γ, CCL3/4, IL-2, XCL-1 and TNF production. (H) Frequency of TRM subsets PD-1-CD103+, PD-1+CD103+ and TEX subsets PD-1+CD103-, PD-1+CD103-CD39+ between control and therapy group. (I) IFN-γ production by TRM and TEX subsets between control and anti-PD-1 therapy group. Wilcoxon test was used in C, F-I. *p <0.05, **p <0.01, ***p <0.001. HCC, hepatocellular carcinoma; OS, overall survival; PD, progressive disease; PFS, progression-free survival; SD, stable disease; TEX, exhausted CD8+ T cells; TILs, tumor-infiltrating lymphocytes; TRM, tissue-resident memory T cells.

These findings relate to the enrichment of peripheral and intratumoral PD-1+ CD8 T cells which stratifies patients with a severe exhaustion phenotype and is associated with poor PFS independent from BCLC stage and AFP levels. The TRM/TEX balance is also linked to patient outcomes during anti-PD-1 therapy and may therefore be useful as an immune biomarker.

An important finding from our study was that PD-1 expression by CD8 T cells alone did not predict patient outcome, irrespective of whether it was determined in the peripheral blood or liver, in contrast to the relative enrichment of PD-1+ cells in the tumor compared to the peripheral blood. Notably, this enrichment was an independent predictor of PFS in multivariate analysis with BCLC stage and AFP levels. Our study highlights that the underlying biology of this novel biomarker depends on the opposing roles for CD103+ TRM and TEX populations in HCC. Core signatures of TRM have been described that include PD-1 expression.[24] Since PD-1 is also an immune checkpoint expressed by exhausted T cells, a careful dissection of exhaustion and residency programs is required that has not been performed in earlier descriptions of residency or exhaustion-related phenotypes in viral etiology HCC cohorts.[8,9,11,17,25] Our study also highlights the utility for single-cell protein-based immune profiling in discriminating TEX and TRM. While exhaustion and transcriptional signatures have been described,[12,26,27] the relevant overlap in gene expression between several TRM and TEX features poses a challenge to discriminate these cell states using gene-set based transcriptional analysis. Here, we found the combined protein expression analysis of adhesion molecule CD103 and PD-1 together with other exhaustion markers helpful to understand the role of TRM vs. TEX in HCC. While not all CD103+ TRM expressed PD-1, the proportion of CD103+PD-1+ TRM among the total PD-1+ TIL clearly correlated with long-term survival. This protective role was associated with better TRM effector function, infiltration of the tumor tissue and reduced co-expression of additional immune checkpoints.

Recent work in murine models of metabolic liver disease mimicking NASH reported that resident-like CD8+PD1+ T cells promote not only NASH but also hepatocarcinogenesis. This effect was further augmented by immunotherapy through increased activation of resident PD-1-expressing CD8 T cells.[13] This notion appears in contrast to the protective role of TRM cells found in our human study. However, in that study, the resident-like character of the cells implicated in NASH progression was not determined by CD103 expression, but rather relied prominently on CXCR6 analysis.[13] While binding of the integrin molecule CD103 to E-cadherin expressed on epithelial cells is important to promote adhesion and retention in the liver and tumor tissue,[28] the role of CXCR6 is largely implicated in the attraction of activated T cells to the liver,[29] which may include precursors of TRM, activated or exhausted T cells. CXCR6 has also been reported to be important for the positioning and survival of CD8 T cells in the tumor microenvironment.[30] Importantly, however, stronger enrichment of exhausted T cells in our study also correlated with NASH etiology, fitting to the notion that exhausted T cells can promote HCC in NASH.[13] Our assessment of the heterogeneity of hepatic and intratumoral TRM phenotypes provides a likely explanation for these seemingly disparate findings, since CD103 expression more clearly defined the non-exhausted TRM population, while CXCR6 and CD69 (in the absence of CD103) could also be expressed by cells with significant features of exhaustion. It will thus be important in future studies to use CD103 in the profiling of hepatic TRM, as the use of CXCR6 and

CD69 may not be sufficient to identify the exhaustion-resistant TRM population.

Moreover, it remained unclear if anti-PD-1 checkpoint blockade preferentially targets protective TRM (as suggested by[8]) or dysfunctional TEX and if these different target cells will have divergent anti-tumor effects. Our analysis of the TEX and TRM ratio in the tumor microenvironment and from the *in vitro* checkpoint therapy model indicates that a high TRM/TEX ratio determines beneficial patient outcomes; however, on a single-cell level, TEX display the strongest functional augmentation after anti-PD-1 therapy. These data suggest that both TRM and TEX can contribute to protective immune function during checkpoint therapy. Interestingly, patients with a high TRM/TEX ratio typically also had a higher intratumoral infiltration of T cells, suggesting a role for immunologically "hot" tumor microenvironments. While further studies are required to address these questions in larger patient cohorts, it is already tempting to speculate that immune checkpoint combination therapies could represent an option to more selectively target TEX cells, as they co-express additional immune checkpoints compared to TRM, and such strategies could synergize with approaches to enhance T-cell infiltration into the tumor.

In sum, our study identifies the dynamics of PD-1-expressing exhausted and resident CD8 T cells as a governing factor of patient outcomes, highlighting these populations as relevant biomarkers of HCC outcomes, with important implications for the monitoring and targeting of these populations during immunotherapy studies.

Abbreviations

AFP, alpha-fetoprotein; ATLs, adjacent non-tumor tissue lymphocyte(s); BCLC, Barcelona Clinic Liver Cancer; CCL3, C-C motif chemokine ligand 3; CTLA-4, cytotoxic T-lymphocyte antigen-4; CXCR6, C-X-C motif chemokine receptor 6; CyTOF, mass cytometry by time of flight; HCC, hepatocellular carcinoma; ICB, immune checkpoint blockade; IFN-γ, interferon-γ; IL-, interleukin-; NASH, non-alcoholic steatohepatitis; OS, overall survival; PBMCs, peripheral blood mononuclear cells; PD-1, programmed cell death 1; PFS, progression-free survival; RT, room temperature; TEX, exhausted CD8+ T cells; TILs, tumor-infiltrating lymphocytes; TRM, tissue-resident memory T cells; t-SNE, t-distributed stochastic neighbor embedding.

Conflict of interest

The authors declare no conflicts of interest. Please refer to the accompanying ICMJE disclosure forms for further details.

Supplementary data

Supplementary data to this article can be found online at https://doi.org/10.1016/j.jhep.2022.02.032.

References

Author names in bold designate shared co-first authorship.

[1] Finn RS, Qin S, Ikeda M, Galle PR, Ducreux M, Kim TT, et al. Atezolizumab plus bevacizumab in unresectable hepatocellular carcinoma. N Engl J Med 2020;382:1894–1905.

[2] Finn RS, Qin S, Ikeda M, Galle PR, Ducreux M, Kim T-Y, et al. IMbrave150: updated overall survival (OS) data from a global, randomized, open-label phase III study of atezolizumab (atezo) + bevacizumab (bev) versus sorafenib (sor) in patients (pts) with unresectable hepatocellular carcinoma (HCC). J Clin Oncol 2021;39. 267-267.

[3] Flecken T, Schmidt N, Hild S, Gostick E, Drognitz O, Zeiser R, et al. Immunodominance and functional alterations of tumor-associated antigen-specific CD8+ T-cell responses in hepatocellular carcinoma. Hepatology 2014;59:1415–1426.

[4] Sia D, Jiao Y, Martinez-Quetglas I, Kuchuk O, Villacorta-Martin C, Castro de Moura M, et al. Identification of an immune-specific class of hepatocellular carcinoma, based on molecular features. Gastroenterology 2017;153:812–826.

[5] Finn RS, Ryoo BY, Merle P, Kudo M, Bouattour M, Lim HY, et al. Pembrolizumab as second-line therapy in patients with advanced hepatocellular carcinoma in KEYNOTE-240: a randomized, double-blind, phase III trial. J Clin Oncol 2020;38:193–202.

[6] Yau T, Park JW, Finn RS, Cheng AL, Mathurin P, Edeline J, et al. Nivolumab versus sorafenib in advanced hepatocellular carcinoma (CheckMate 459): a randomised, multicentre, open-label, phase 3 trial. Lancet Oncol 2022;23:77–90.

[7] McLane LM, Abdel-Hakeem MS, Wherry EJ. CD8 T cell exhaustion during chronic viral infection and cancer. Annu Rev Immunol 2019;37:457–495.

[8] Chew V, Lai L, Pan L, Lim CJ, Li J, Ong R, et al. Delineation of an immunosuppressive gradient in hepatocellular carcinoma using high-dimensional proteomic and transcriptomic analyses. Proc Natl Acad Sci USA 2017;114:E5900–E5909.

[9] **Lim CJ**, **Lee YH**, Pan L, Lai L, Chua C, Wasser M, et al. Multidimensional analyses reveal distinct immune microenvironment in hepatitis B virus-related hepatocellular carcinoma. Gut 2018;68.

[10] Kim HD, Park S, Jeong S, Lee YL, Lee H, Kim CG, et al. 4-1BB delineates distinct activation status of exhausted tumor-infiltrating CD8+ T cells in hepatocellular carcinoma. Hepatology 2020;71:955–971.

[11] Kim HD, Song GW, Park S, Jung MK, Kim MH, Kang HJ, et al. Association between expression level of PD1 by tumor-infiltrating CD8+ T cells and features of hepatocellular carcinoma. Gastroenterology 2018;155:1936–1950.e17.

[12] Bengsch B, Ohtani T, Khan O, Setty M, Manne S, O'Brien S, et al. Epigenomic-guided mass cytometry profiling reveals disease-specific features of exhausted CD8 T cells. Immunity 2018;48:1029–1045 e1025.

[13] Pfister D, Núñez NG, Pinyol R, Govaere O, Pinter M, Szydlowska, et al. NASH limits anti-tumour surveillance in immunotherapy-treated HCC. Nature 2021;592:450–456.

[14] Dudek M, Pfister D, Donakonda S, Filpe P, Schneider A, Laschinger M, et al. Auto-aggressive CXCR6 + CD8 T cells cause liver immune pathology in NASH. Nature 2021;592:444–449.

[15] Pinato DJ, Marron TU, Mishra-Kalyani PS, Gong Y, Wei G, Szafron D, et al. Treatment-related toxicity and improved outcome from immunotherapy in hepatocellular cancer: evidence from an FDA pooled analysis of landmark clinical trials with validation from routine practice. Eur J Cancer 2021;157:140–152.

[16] Winkler F, Bengsch B. Use of mass cytometry to profile human T cell exhaustion. Front Immunol 2020;10:3039.

[17] **Ma J**, **Zheng B**, **Goswami S**, **Meng L**, Zhang D, Cao C, et al. PD1Hi CD8+ T cells correlate with exhausted signature and poor clinical outcome in hepatocellular carcinoma. J Immunother Cancer 2019;7:331.

[18] Cancer Genome Atlas Research Network. Electronic address wbe, cancer Genome atlas research N. Comprehensive and integrative genomic characterization of hepatocellular carcinoma. Cell 2017;169:1327–1341 e1323.

[19] Szabo PA, Miron M, Farber DL. Location, location, location: tissue resident memory T cells in mice and humans. Sci Immunol 2019;4:eaas9673.

[20] **Zheng C**, **Zheng L**, **Yoo JK**, Guo H, Zhang Y, Guo X, et al. Landscape of infiltrating T cells in liver cancer revealed by single-cell sequencing. Cell 2017;169:1342–1356.e1316.

[21] Blackburn SD, Shin H, Haining WN, Zou T, Workman CJ, Polley A, et al. Coregulation of CD8+ T cell exhaustion during chronic viral infection by multiple inhibitory receptors. Nat Immunol 2009;10:29–37.

[22] Bengsch B, Johnson AL, Kurachi M, Odorizzi PM, Pauken KE, Attansio J, et al. Bioenergetic insufficiencies due to metabolic alterations regulated by PD-1 are an early driver of CD8+ T cell exhaustion. Immunity 2016;45:358–373.

[23] Pan Y, Tian T, Park CO, Lofftus SY, Mei S, Li X, et al. Survival of tissue-resident memory T cells requires exogenous lipid uptake and metabolism. Nature 2017;543:252–256.

[24] Kumar BV, Ma W, Miron M, Granot T, Guyer RS, Carpenter DJ, et al. Human tissue-resident memory T cells are defined by Core transcriptional and functional signatures in lymphoid and mucosal sites. Cell Rep 2017;20:2921–2934.

[25] Cheng Y, Gunasegaran B, Singh HD, Dutertre CA, Loh CY, Lim JQ, et al. Non-terminally exhausted tumor-resident memory HBV-specific T cell responses correlate with relapse-free survival in hepatocellular carcinoma. Immunity 2021;54:1825–1840.e7.

[26] MacKay LK, Rahimpour A, Ma JZ, Collins N, Stock AT, Hafon ML, et al. The developmental pathway for CD103+ CD8+ tissue-resident memory T cells of skin. Nat Immunol 2013;14:1294–1301.

[27] **Pritykin Y**, **van der Veeken J**, Pine AR, Zhong Y, Sahin M, Mazutis L, et al. A unified atlas of CD8 T cell dysfunctional states in cancer and infection. Mol Cel 2021;81:2477–2493.e2410.

[28] Le Floc'h A, Jalil A, Franciszkiewicz K, Validire P, Vergnon I, Mami-Chouaib F. Minimal engagement of CD103 on cytotoxic T lymphocytes with an E-cadherin-Fc molecule triggers lytic granule polarization via a phospholipase Cgamma-dependent pathway. Cancer Res 2011;71:328–338.

[29] **Sato T**, **Thorlacius H**, Johnston B, Staton TL, Xiang W, Littman DR, et al. Role for CXCR6 in recruitment of activated CD8+ lymphocytes to inflamed liver. J Immunol 2005;174:277–283.

[30] **Di Pilato M**, **Kfuri-Rubens R**, **Pruessmann JN**, **Ozga AJ**, Messemaker M, Cadilha BL, et al. CXCR6 positions cytotoxic T cells to receive critical survival signals in the tumor microenvironment. Cell 2021;184:4512–4530. e4522.